METAL FORMING ANALYSIS BY FOURIER SERIES EXPANSION AND FURTHER USES OF PSEUDO–CONCENTRATIONS

H. J. ANTÚNEZ †, S. R. IDELSOHN ‡
Computational Mechanics Laboratory of INTEC
(University of Litoral and CONICET)
P. O. Box 91 — 3000 Santa Fe – Argentina
E. N. DVORKIN §
Center for Industrial Research, FUDETEC Argentina

ABSTRACT

An analysis of metal forming processes with axial geometry is performed by an expansion in Fourier Series on the circumferential direction. For that purpose, an incremental form is presented on the basis of the flow formulation. For every increment of the non–null imposed boundary conditions an algebraic system is formed in which the non–linearity due to the visco–plastic properties of the material is placed as part of the load term. In this way, the global stiffness matrix is block diagonal, the coupling due to material non–linearity being included in the right hand side. Free surfaces are treated as an interface inside the elements, as an extension of the pseudo–concentration method.

1. INTRODUCTION

A large variety of processes can be easily treated with a 2–D model, i.e. those where plane stress state or axisymmetric configurations are had. However, there are also many situations in which a full 3–D analysis is required. In some of these cases this can be achieved by a semi–analytical method through an Fourier series expansion along one direction. The application of this method is straightforward when dealing with linear problems [1,2], in which a decoupling of the modal components is held, due to the orthogonal properties of trigonometric functions. The solution of non–linear problems has been reached for particular cases, trying to produce the uncoupling of the modal components so as to solve the three dimensional problem as a combination of a number of two dimensional

† Senior Research Assistant (CONICET)
‡ Professor and Scientific Researcher
§ Senior Research Engineer

ones. Besides, in metal forming problems the flow formulation has provided a simple and effective way of dealing with metal forming processes. Its application has been mostly in 2-D situations, and where elastic deformations are negligible. In this work we present a semi-analytical method to deal with metal forming processes in terms of the flow formulation.

Furthermore, among various methods to model transient metal forming processes, the pseudo-concentration method has proved to be efficient, simple and accurate. It basically consists of treating free surfaces as interfaces between two media, the metal and a fictitious material with mechanical and thermal properties conveniently assigned, so as not to disturb the flow of metal. We make use of this artifice to model the non-axisymmetric free surface keeping a consistent structure to allow the series expansion.

The incremental formulation is shown in first place. Then the element with the series expansion is developed, and the extension of the pseudo-concentration method for non axisymmetric free surface handling is shown. Finally some numerical applications are included to check the performance of the model.

2. INCREMENTAL FORMULATION

a) Explicit form

The flow formulation makes use of an Eulerian approach so that, although there are large deformations in the processes being modeled, they do not affect in the non-linearity of the problem, which is due only to the constitutive equation (material non-linearity). The typical effective strain rate vs. effective stress curve is supposed to be formed by small straight lines (fig. 1).

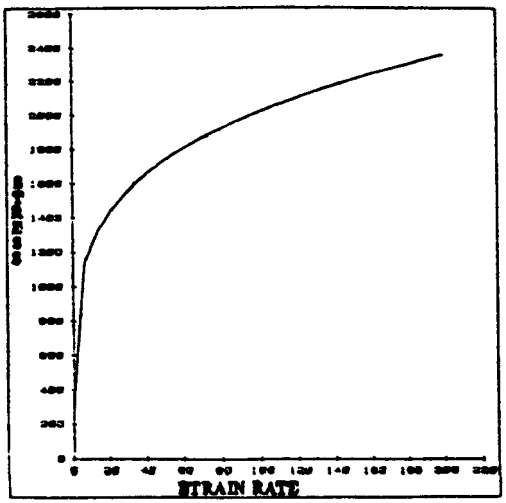

Figure 1. Strain rate vs stress for a typical visco-plastic material

The problem is formulated in the non-linear form in terms of the principle of virtual velocities

$$\int_\Omega \delta\dot{\varepsilon}_{ij}\sigma_{ij}d\Omega - \int_\Omega \delta u_i \rho\left(P_i - \frac{\partial u_i}{\partial t} - u_j u_{i,j}\right)d\Omega - \int_{\Gamma_T} \delta u_i T_i d\Gamma = 0 \qquad (1)$$

which, after neglecting dynamic and inertial terms, and by requiring incompressibility condition, is equivalent to require stationarity of

$$\int_\Omega \dot{\varepsilon}_{ij} 2\mu\dot{\varepsilon}_{ij}d\Omega - \int_\Omega \dot{\varepsilon}_{ij} p\delta_{ij}d\Omega - \int_\Gamma u_i T_i d\Gamma = 0. \qquad (2)$$

with respect to any virtual velocity variation, and vanishing the power due to hydrostatic deformation

$$\int_\Omega \delta p\, \dot{\varepsilon}_{ii}d\Omega = 0. \qquad (3)$$

Taking variations and requiring stationarity of the governing functionals yields, for a single element

$$\begin{bmatrix} \mathbf{K} & \mathbf{K}_p^T \\ \mathbf{K}_p & \mathbf{0} \end{bmatrix} \begin{Bmatrix} \mathbf{u}^N \\ p^N \end{Bmatrix} = \begin{Bmatrix} \mathbf{F}_u \\ \mathbf{0} \end{Bmatrix}, \qquad (4)$$

where

$$\mathbf{K} = \int_\Omega \mathbf{B}^T \mu \mathbf{D}\mathbf{B}d\Omega, \qquad (5)$$

and

$$\mathbf{K}_p = -\frac{1}{2}\int_\Omega \mathbf{N}_p^T \mathbf{I}\mathbf{B}d\Omega. \qquad (6)$$

Here is B such that $\underline{\dot{\varepsilon}} = \mathbf{B}\mathbf{u}$, D, such that $\underline{s} = \mu\mathbf{D}\underline{\dot{\varepsilon}}$, and I such that $\dot{\varepsilon}_v = \mathbf{I}\underline{\dot{\varepsilon}}$. For the plane case is $\mathbf{I} = \lfloor 1 \quad 1 \quad 0 \rfloor$.

In the incremental formulation we have

$$\begin{aligned} \{\mathbf{u}_{n+1}^N\} &= \{\mathbf{u}_n^N + \Delta\mathbf{u}_n^N\} \\ \{p_{n+1}^N\} &= \{p_n^N + \Delta p_n^N\} \end{aligned}, \qquad (7)$$

so that

$$\begin{aligned} \delta\{\mathbf{u}_{n+1}^N\} &= \delta\{\Delta\mathbf{u}_n^N\} \\ \delta\{p_{n+1}^N\} &= \delta\{\Delta p_n^N\} \end{aligned}, \qquad (8)$$

the values of $\mathbf{u}_n^N$ and p_n^N act as an initial condition when passing from load step n to $n+1$. For the first step a constant viscosity is introduced.

Therefore, the system will be

$$\begin{bmatrix} \mathbf{K} & \mathbf{K}_p^T \\ \mathbf{K}_p & \mathbf{0} \end{bmatrix} \begin{Bmatrix} \Delta\mathbf{u}_n^N \\ \Delta p_n^N \end{Bmatrix} = \begin{Bmatrix} \mathbf{F}_{u_n} \\ \mathbf{0} \end{Bmatrix} - \begin{bmatrix} \mathbf{K} & \mathbf{K}_p^T \\ \mathbf{K}_p & \mathbf{0} \end{bmatrix} \begin{Bmatrix} \mathbf{u}_n^N \\ p_n^N \end{Bmatrix}. \qquad (9)$$

The right hand side computes the load due to the initial rate of deformation for the present increment. Therefore, for analogy with other methods [3], this incremental formulation can be called the *initial strain rate method*.

In this system of equations the viscosity, which multiplies the matrix K_0 is a function of the velocity field. Its value in each point is supposed to be constant throughout the load increment, having been calculated at the beginning of it. This hypothesis will be acceptable when the load increment is sufficiently small, and here is the linearization of the viscoplastic flow problem. As regards the length of these steps, Cormeau [4] has studied the critical value that assures the stability of this type of integration schemes.

By this procedure and, when taking a sufficient number of steps, an acceptable precision can be achieved compared to the full non-linear solution. This has been tested calculating the normalized residual with the solution yielded by the incremental scheme. Table *I* shows these values for various numbers of steps, for a direct extrusion case, modeled with nine elements.

Table *I*

Number of steps	Norm. Res.	CPU(min:sec)
3	0.03493	1:08
5	0.01907	1:34
8	0.01129	2:10
10	0.00890	2:40

It should be pointed out that in addition, this scheme is suitable to deal with perfectly plastic materials, where the tangent stiffness matrix is singular: infinitely large velocities increments would be obtained for a given increase in the external loads. Therefore, a Newton-Raphson scheme cannot be applied [5], and when solved by a back-substitution procedure, a great number of iterations is required to achieve convergence of the algebraic system.

This scheme also allows the treatment of free surfaces, as shown in the following section, this being very interesting because the generality of the method is conserved.

b) Extension to cases with free surfaces

It is well known that, in metal forming processes, several free surfaces are usually encountered. Thus, the final form of a stationary process is included in what has to be found out. Due to this factor, a non-linearity inside each increment appears. When imposing the free surface condition, velocity increments not tangent to the surface can be obtained. If the coordinates of the nodes are then modified in order to fulfill this condition, one has that although the velocity field has not changed, the geometry of the domain has. Then it is necessary to recalculate the global stiffness matrix so as to have new displacements values. With them, the nodal coordinates are newly adjusted, and iterations continue until convergence is achieved. For the i^{th} iteration we define the residual

$$R = \sum_{k=1}^{N_{SL}} \left(\frac{u_k}{v_k} - m_k \right)^2 , \qquad (10)$$

and the norm

$$N = \sum_{k=1}^{N_{SL}} \left(\frac{u_k}{v_k}\right)^2, \tag{11}$$

where

N_{SL} number of nodes of the free surface,
m_k slope of the tangent to the domain on node k,
u_k, v_k velocity components of node k,
and the sub-iterations are continued until

$$\frac{R}{N} < \delta, \tag{12}$$

where δ is the convergence tolerance.

However, being the variations in geometry for each load increment small, a modified Newton scheme can be proposed for the iterations within the step. This means using an equal tangent matrix on it. In this way in each iteration the residual is recalculated but the global matrix is not triangularized. This hypotheses is supported on the fact that the non-linearity associated to the free surfaces is a mild one; the velocity field is fixed with respect to the nodes, and so, in fact, convergence of the sub-problem is achieved within the first three iterations. Each one of them requires, in case this simplification is not assumed, the full solution of the equations system. Time saving due to the adoption of the quasi-Newton scheme is considerable.

A further step in simplificating assumptions consists of linearizing this non-linear sub-problem as well, assuming that the geometry found by integration of the free surfaces is such that the velocity increments calculated on the basis of that geometry fulfill the free surface boundary conditions. This is equivalent to eliminating every sub-iteration in the load increments. Again, the results of this simplifications are very encouraging. They are evaluated by calculating the normalized residual in terms of the incremental solution, on the non-linear system of equations.

It can be seen that the approximation made to linearize this problem is at most of the same order than that made to reach the incremental form. So the method converges linearly with the number of load steps, even when simultaneous treatment of free surfaces is considered. When the number of load steps is increased, the differences between the three methods tested lowers, until it is not appreciated, generally, from number of load steps greater than 20.

c) The implicit incremental scheme

The aim of the present section is to be able to express the flow formulation in such a way that a Fourier expansion may be possible. It is then necessary to have a stiffness matrix non-dependent on the circumferential coordinate. But, as the viscosity, which is a factor of a sub-matrix of the stiffness matrix, is a function of the rate of deformation, an implicit iterative scheme has to be used, in order to achieve this condition, taking as an equivalent load part of the product of the complete matrix by the approximate solution vector.

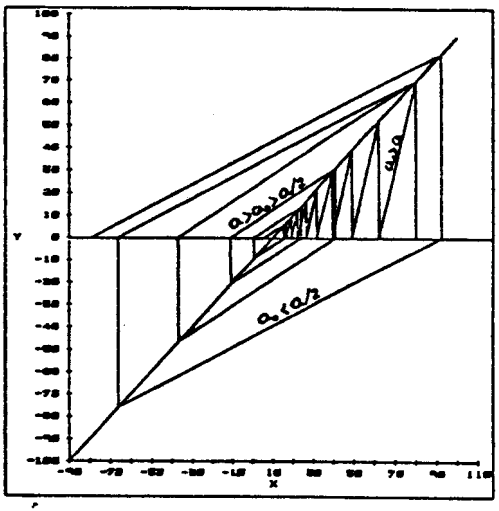

Figure 2. One–dimensional scheme for the incremental algorithm

Let us consider the solution of a linear equation with a single unknown

$$ax + b = 0. \tag{13}$$

If we express the coefficient a as $a = a_0 + a_1$, we can say

$$x = -\frac{b}{a_0} - \frac{a_1}{a_0}x. \tag{14}$$

This expression can be used in an iterative process writing

$$x_{n+1} = -\frac{b}{a_0} - \frac{a_1}{a_0}x_n. \tag{15}$$

The solution of (13) is reached when

$$|x_{n+1} - x_n| < \delta, \tag{16}$$

where δ is a tolerance of convergence.

The solution procedure is represented in Fig. 2, from which the following observations can be made

1) for convergence of the algorithm it is required that $a_0 > a/2$. If $a_0 = a/2$, numerical solution oscillates between to values at a same distance from the exact solution, and if $a_0 < a/2$ the algorithm diverges.
2) convergence is faster as a_0 approximates a.
3) for values of a_0 greater than a there is no limitation on convergence, but it is desirable to have a_0 as low as possible, for the reason pointed out in 2)
4) the numerical solutions make a monotonically succession when $a_0 > a$, while it is alternated if $a > a_0 > a/2$
5) clearly, if $a_0 = a$ the exact solution is reached in a single step.

By means of this procedure we analyze the possibility of reaching the solution if the coefficient of the unknown is non–constant and it is desired to iterate with a constant slope. When extending this solution scheme to the visco–plastic flow problem with Fourier series expansion we will have a coefficient matrix non–dependent on the circumferential direction, remaining the variable component of the matrix as part of the load term. This condition of matrix non–dependent on the circunferential direction is necessary to allow the series expansion, with the uncoupling of the modes in the global stiffness matrix.

On considering the visco–plastic problem, the viscosity is written

$$\mu = \mu' + \mu_M, \tag{17}$$

where $\mu = \mu(\mathbf{x})$, $\mu' = \mu'(\mathbf{x})$, and $\mu_M = constant$, and $\mathbf{x}$ is the position vector. In what follows we introduce this notation: by defining the matrix $\mathbf{K}_0 = \int_\Omega \mathbf{B}^T\mathbf{D}\mathbf{B}d\Omega$, we will refer to K (equation (5)), as $\mathbf{K} = \mu\mathbf{K}_0$. Although μ depends on the position vector, we denote the use of different definitions of viscosity (which is is a factor in the integrand), as the product of that viscosity by the matrix $\mathbf{K}_0$, which only depends on geometric factors. The implicit incremental scheme results in

$$\begin{bmatrix} \mu_{M_n}\mathbf{K}_0 & \mathbf{K}_p^T \\ \mathbf{K}_p & \mathbf{0} \end{bmatrix} \begin{Bmatrix} \Delta\mathbf{u}_n^k \\ \Delta p_n^k \end{Bmatrix} = \begin{Bmatrix} \mathbf{F}_{n_n} \\ \mathbf{0} \end{Bmatrix} - \begin{bmatrix} \mu_n\mathbf{K}_0 & \mathbf{K}_p^T \\ \mathbf{K}_p & \mathbf{0} \end{bmatrix} \begin{Bmatrix} \mathbf{u}_n^k \\ p_n^k \end{Bmatrix} - \begin{bmatrix} \mu'_n\mathbf{K}_0 & \mathbf{0} \\ \mathbf{0} & \mathbf{0} \end{bmatrix} \begin{Bmatrix} \Delta\mathbf{u}_n^{k-1} \\ \Delta p_n^{k-1} \end{Bmatrix}. \tag{18}$$

It is required, to assure convergence, that

$$\left\| \begin{bmatrix} \mu_{M_n}\mathbf{K}_0 & \mathbf{K}_p^T \\ \mathbf{K}_p & \mathbf{0} \end{bmatrix}^{-1} \right\| \cdot \left\| \begin{bmatrix} (\mu_n - \mu_{M_n})\mathbf{K}_0 & \mathbf{0} \\ \mathbf{0} & \mathbf{0} \end{bmatrix} \right\| < 1, \tag{19}$$

This condition is automatically fulfilled if we take

$$\mu_{M_n} = \max_{i=1,N_E} \mu_i, \tag{20}$$

where μ_i is the average viscosity on i^{th} element, and N_E the total number of elements. It is not required to take the absolute maximum viscosity throughout the whole domain, and this is convenient in order to approximate the product of the matrix norms (19) to unity, this condition allows a faster convergence of the algorithm. It should be noted that element matrices are evaluated only at the beginning of every load step; afterwards it is only necessary to evaluate the right hand side of (18). Moreover, the inversion of the global stiffness matrix can be avoided in the steps after the first one, by proper scaling of the first inverted matrix. This helps to save computing time.

3. SEMI–ANALYTICAL FORMULATION

This section deals with the three–dimensional, axisymmetric in geometry problem. We consider arbitrary loads and boundary conditions. A Fourier

series expansion is performed in the circumferential direction. Previous steps of linearization and stating the problem with a constant stiffness matrix were aimed at to make the following development possible.

There are two objectives, namely the element matrices generation, and the evaluation of the load terms.

According to the solution strategy proposed, we seek to solve as many uncoupled systems of equations as base functions are taken to make the series expansion. As it has already been shown, the problem has been transformed so as to have constant coefficient matrices, non-dependent on the azimuthal coordinate. This has been at the cost of solving in an implicit way, and thus, iteratively, a problem which in absence of the series expansion would be explicit and linear, due to the small increments taken when imposing the loads.

To achieve the uncoupled solution of the modes we have to compute the right hand side for each mode considering the contribution of every mode. In this way the coupling due to the non-linear nature of the visco-plastic material is considered, without losing the uncoupling of the equations system to be solved in each iteration.

In the present configuration the rate of deformation tensor is written in cylindrical coordinates

$$\begin{Bmatrix} \dot{\epsilon}_r \\ \dot{\epsilon}_z \\ \dot{\epsilon}_\theta \\ \dot{\epsilon}_{rz} \\ \dot{\epsilon}_{z\theta} \\ \dot{\epsilon}_{\theta r} \end{Bmatrix} = \begin{Bmatrix} \frac{\partial u}{\partial r} \\ \frac{\partial v}{\partial z} \\ \frac{u}{r} + \frac{1}{r}\frac{\partial w}{\partial \theta} \\ \frac{\partial u}{\partial z} + \frac{\partial v}{\partial r} \\ \frac{1}{r}\frac{\partial u}{\partial \theta} + \frac{\partial w}{\partial r} - \frac{w}{r} \\ \frac{1}{r}\frac{\partial v}{\partial \theta} + \frac{\partial w}{\partial z} \end{Bmatrix}. \tag{21}$$

By geometric considerations, it is convenient to define the series expansion of the velocity components as follows

$$\begin{pmatrix} u \\ v \\ w \end{pmatrix} = \begin{pmatrix} u_0 \\ v_0 \\ w_0 \end{pmatrix} + \sum_{l=1}^{L} \left[\begin{pmatrix} u_l \cos l\theta \\ v_l \cos l\theta \\ w_l \sin l\theta \end{pmatrix} + \begin{pmatrix} -u_{-l} \sin l\theta \\ -v_{-l} \sin l\theta \\ w_{-l} \cos l\theta \end{pmatrix} \right]. \tag{22}$$

This form results from considering that a symmetric load directed along the r or z coordinates will yield symmetric displacements along r and z, but antisymmetric along θ, the converse occurring with symmetric load directed along θ. This fact, together with the signs adopted yield a global system that is uncoupled in the harmonic components, and in a single harmonic, the u^l component is uncoupled with respect to the u^{-l}. Finally, as will be shown in what follows, the matrices for both components of a same harmonic are identical. This reduces the time required for its evaluation and resolution. There are, so, $2L+1$ systems of dimension $N \times N$, where N is the number of degrees of freedom for each harmonic component, where there are only $L+1$ matrices to calculate and invert.

This grouping of the two phases of the velocity components into a single mode l (which we will denote with a positive and negative subindex, respectively)

is taken into account by definition of the matrices

$$\begin{aligned} \mathbf{I}^l &= \begin{pmatrix} \cos l\theta & 0 & 0 \\ 0 & \cos l\theta & 0 \\ 0 & 0 & \sin l\theta \end{pmatrix} \\ \mathbf{K}^l &= \begin{pmatrix} \sin l\theta & 0 & 0 \\ 0 & \sin l\theta & 0 \\ 0 & 0 & -\cos l\theta \end{pmatrix} \end{aligned} \tag{23}$$

(more precisely, each element of $\mathbf{I}^l$ and $\mathbf{K}^l$ is a diagonal matrix of order equal to the number of nodes of the element). So, we can rewrite (22) as

$$\mathbf{u} = \mathbf{u}_0 + \sum_{l=1}^{L} \left(\mathbf{u}_l \mathbf{I}^l - \mathbf{u}_{-l} \mathbf{K}^l \right) \tag{24}$$

We can also express the strain rate tensor as the sum of the contributions of each harmonic component

$$\{\dot{\epsilon}\} = \{\dot{\epsilon}\}_0 + \sum_{l=1}^{L} \left(\{\dot{\epsilon}\}_l + \{\dot{\epsilon}\}_{-l} \right) \tag{25}$$

where

$$\{\dot{\epsilon}\}_0 = \mathbf{B}_0 \mathbf{u}_0 \tag{26}$$

$$\{\dot{\epsilon}\}_l = \left(\mathbf{B}_0 \mathbf{I}^l - l\hat{\mathbf{B}} \mathbf{K}^l \right) \mathbf{u}_l \tag{27}$$

$$\{\dot{\epsilon}\}_{-l} = \left(-\mathbf{B}_0 \mathbf{K}^l - l\hat{\mathbf{B}} \mathbf{I}^l \right) \mathbf{u}_{-l} \tag{28}$$

where, from (21) and (22) results

$$\mathbf{B}_0 = \begin{bmatrix} \frac{\partial \mathbf{N}_u}{\partial r} & 0 & 0 \\ 0 & \frac{\partial \mathbf{N}_u}{\partial z} & 0 \\ \frac{\mathbf{N}_u}{r} & 0 & 0 \\ \frac{\partial \mathbf{N}_u}{\partial z} & \frac{\partial \mathbf{N}_u}{\partial r} & 0 \\ 0 & 0 & \frac{\partial \mathbf{N}_u}{\partial r} - \frac{\mathbf{N}_u}{r} \\ 0 & 0 & \frac{\partial \mathbf{N}_u}{\partial z} \end{bmatrix} \tag{29}$$

and

$$\hat{\mathbf{B}} = \frac{\mathbf{N}_u}{r} \begin{bmatrix} 0 & 0 & 0 \\ 0 & 0 & 0 \\ 0 & 0 & 1 \\ 0 & 0 & 0 \\ 1 & 0 & 0 \\ 0 & 1 & 0 \end{bmatrix} \tag{30}$$

When talking about harmonic components of the velocity, we will refer in what follows to their nodal values, so that, for easiness of notation, the superindex N will be omited.

Equations (26) to (28) define the matrix B, relating velocities with strain rates. It will be

$$\{\dot{\varepsilon}\} = \mathbf{B}\{\mathbf{u}\} = [\mathbf{B}_0 \quad \mathbf{B}_1 \quad \mathbf{B}_{-1} \quad \dots \quad \mathbf{B}_L \quad \mathbf{B}_{-L}] \begin{Bmatrix} \mathbf{u}_0 \\ \mathbf{u}^1 \\ \mathbf{u}^{-1} \\ \vdots \\ \mathbf{u}^L \\ \mathbf{u}^{-L} \end{Bmatrix}. \tag{31}$$

On application of virtual velocities, terms of the type

$$\delta \left[\int_\Omega \{\dot{\varepsilon}\}^T_{\pm i} \mu \mathbf{D} \{\dot{\varepsilon}\}_{\pm j} \, d\Omega - \int_\Omega \{\dot{\varepsilon}\}^T_{\pm i} \mathbf{I} \{p_j\} \, d\Omega - \int_\Omega \{\mathbf{u}\}^T_{\pm i} \mathbf{F}_j d\Omega \right] = 0, \tag{32}$$

will be obtained, with sum on j and where i, j vary from 1 to L.

For the 3–D case we have

$$\mathbf{I} = [1 \quad 1 \quad 1 \quad 0 \quad 0 \quad 0] \tag{33}$$

and

$$\mathbf{D} = \begin{bmatrix} 2 & & & & & \\ & 2 & & & 0 & \\ & & 2 & & & \\ & & & 1 & & \\ & 0 & & & 1 & \\ & & & & & 1 \end{bmatrix} \tag{34}$$

By considering the orthogonallity of the basis functions of a Fourier series results

$$\begin{aligned} &\int_0^{2\pi} d\theta = 2\pi \\ &\int_0^{2\pi} \sin i\theta d\theta = \int_0^{2\pi} \cos i\theta d\theta = 0 \\ &\int_0^{2\pi} \cos i\theta \cos j\theta d\theta = \int_0^{2\pi} \sin i\theta \sin j\theta d\theta = \begin{cases} \pi & \text{if } i = j \\ 0 & \text{if } i \neq j \end{cases} \\ &\int_0^{2\pi} \sin i\theta \cos j\theta d\theta = 0, \end{aligned} \tag{35}$$

from which equation (32) yields a block diagonal coefficient matrix such that, for $i = j$

$$\mathbf{K}_{ij} = \pi \begin{bmatrix} \int_A (\mathbf{B}_0^T \mu_M \mathbf{D} \mathbf{B}_0 - j(\mathbf{B}_0^T \mu_M \mathbf{D} \hat{\mathbf{B}})^* & 0 \\ -i(\hat{\mathbf{B}}^T \mu_M \mathbf{D} \mathbf{B}_0)^* + ij \hat{\mathbf{B}}^T \mu_M \mathbf{D} \hat{\mathbf{B}}) dA & \\ 0 & \int_A (\mathbf{B}_0^T \mu_M \mathbf{D} \mathbf{B}_0 - j(\mathbf{B}_0^T \mu_M \mathbf{D} \hat{\mathbf{B}})^* \\ & -i(\hat{\mathbf{B}}^T \mu_M \mathbf{D} \mathbf{B}_0)^* + ij \hat{\mathbf{B}}^T \mu_M \mathbf{D} \hat{\mathbf{B}}) dA \end{bmatrix} \tag{36}$$

where

$$\mathbf{M}^* = \mathbf{M}\mathbf{L} \tag{37}$$

and

$$\mathbf{L} = \begin{pmatrix} 1 & 0 & 0 \\ 0 & 1 & 0 \\ 0 & 0 & -1 \end{pmatrix} \tag{38}$$

In addition, matrices $\mathbf{K}_p$ and $\mathbf{K}_p^T$ are computed. They stand for incompressibility condition and the second term of (32). Similarly, the pressure p has been expanded

$$p = p_0 + \sum_{l=1}^{L} \left(p^l \cos l\theta - p^{-l} \sin l\theta \right). \tag{39}$$

By an analogous procedure we obtain

$$\mathbf{K}_{p_{ij}} = \pi \delta_{ij} \begin{bmatrix} \mathbf{K}_{0_p}^j & 0 \\ 0 & \mathbf{K}_{0_p}^j \end{bmatrix} \tag{40}$$

where

$$\mathbf{K}_{0_p}^j = \begin{pmatrix} \mathbf{N}_p^T(\mathbf{N}_{u,r} + \mathbf{N}_u/r) & \mathbf{N}_p^T \mathbf{N}_{u,z} & j\mathbf{N}_p^T \mathbf{N}_u/r \end{pmatrix} \tag{41}$$

Again, a same matrix is had for both components of the i^{th} harmonic.

As already mentioned, the preceding evaluation of a block diagonal matrix requires the computation of the coupling due to the material non-linearity as an equivalent load. As the real viscosity is non-constant on θ, the difference between a constant value μ_M will have to be integrated along θ, and the orthogonallity properties will not be useful any longer.

According to section 1.c there has to be evaluated the load vector

$$\mathbf{F} = \begin{Bmatrix} \mathbf{F}_{u_n} \\ 0 \end{Bmatrix} - \begin{bmatrix} \mu \mathbf{K}_0 & \mathbf{K}_p^T \\ \mathbf{K}_p & 0 \end{bmatrix} \begin{Bmatrix} \mathbf{u}_n \\ p_n \end{Bmatrix} - \begin{bmatrix} (\mu - \mu_M)\mathbf{K}_0 & 0 \\ 0 & 0 \end{bmatrix} \begin{Bmatrix} \Delta \mathbf{u}_n^{i-1} \\ \Delta p_n^{i-1} \end{Bmatrix} \tag{42}$$

Unlike the 2-D implicit incremental case, the degrees of freedom of the problem are now the harmonic components of nodal velocities and pressures. Looking at the matrices we see that, being μ a function of the circumferential coordinate, the global matrix will not be block diagonal, but there will be a coupling of the modes: to evaluate the independent term of a mode it is necessary to compute also the contribution of the other modes. In order to calculate the integrals on θ we evaluate these independent terms in different angles, making then a numerical integration by a Gaussian quadrature rule. We remark that this coupling does not extend to the global matrix of the system to be solved, so each harmonic will be solved independently.

For the first term of (42), in what concerns the degrees of freedom corresponding to velocities, it can be seen that it is only necessary to evaluate a few simple matrices, namely

$$I_1 = \int_A 2\mu \mathbf{N}_{,r}^T \mathbf{N}_{,r} dA \tag{43a}$$

$$I_2 = \int_A \mu \mathbf{N}_{,r}^T \mathbf{N}_{,z} dA \tag{43b}$$

$$I_3 = \int_A 2\mu \mathbf{N}_{,z}^T \mathbf{N}_{,z} dA \tag{43c}$$

$$I_4 = \int_A 2\mu \frac{\mathbf{N}^T}{r}\frac{\mathbf{N}}{r} dA \tag{43d}$$

$$I_5 = \int_A \mu \frac{\mathbf{N}^T}{r}(\mathbf{N}_{,r} - \frac{\mathbf{N}}{r}) dA \tag{43e}$$

$$I_6 = \int_A \mu \frac{\mathbf{N}^T}{r} \mathbf{N}_{,z} dA \tag{43f}$$

so we will have, for instance, and recalling the notation introduced in (24) to (28)

$$\int_A \mathbf{I}^i \mathbf{B}_0^T \mu \mathbf{D} \mathbf{B}_0 \mathbf{I}^j dA$$

$$= \begin{bmatrix} (I_1+I_4+I_5/2)\cos i\theta \cos j\theta + I_4/2 i \sin i\theta j \sin j\theta & I_2 \cos i\theta \cos j\theta & -I_5 i \sin i\theta \cos j\theta - I_4 \cos i\theta j \sin j\theta \\ I_2^T \cos i\theta \cos j\theta & (I_3+I_1/2)\cos i\theta \cos j\theta + I_4/2 i \sin i\theta j \sin j\theta & -I_6 i \sin i\theta \cos j\theta \\ -I_5^T \cos i\theta j \sin j\theta - I_4 i \sin i\theta \cos j\theta & -I_6^T \cos i\theta j \sin j\theta & (I_1/2 - I_3^T - I_5 - I_4/2)\cos i\theta \cos j\theta + I_4 i \sin i\theta j \sin j\theta \end{bmatrix} \tag{44}$$

It should be noted that the viscosity, being a function of the velocity field, is constant throughout each load step. Therefore, the first term in (42) is constant, and the second term is re–evaluated by simple matrix products. Only for $l = k$ the matrix

$$\begin{bmatrix} \mu_M \mathbf{K}_0 & 0 \\ 0 & 0 \end{bmatrix}$$

will be non–zero, so the subtraction will be necessary only in these cases.

As regards the terms corresponding to the pressure, it can be seen that for being linear their derivation is straightforward and yields

$$\mathbf{F}_1^{up}{}_{ij} = \pi \delta_{ij} \begin{bmatrix} \mathbf{K}_{0p}^j & 0 \\ 0 & \mathbf{K}_{0p}^j \end{bmatrix} \cdot \begin{Bmatrix} p_j \\ p_{-j} \end{Bmatrix} \tag{45}$$

where $\mathbf{K}_{0p}^j$ has been obtained in (41). The derivation for the reciprocal contribution, $\mathbf{F}_1^{pu}{}_{ij}$ is fully analogous.

4. FREE SURFACES BY PSEUDO–CONCENTRATIONS

The transient forming processes modelled with the flow formulation [6] have firstly been solved by Lagrangian approaches [6,7] with moving meshes attached to the material, involving the typical drawbacks of these procedures, namely errors due to element distortion, and remeshing. Thompson [S] has proposed a method by which transient problems are handled in terms of an Eulerian approach with no distortion of the elements. Free surfaces, corresponding to free moving boundaries are treated as an interface of it with a fictitious material whose physical (*i.e.* viscoplastic and thermal) properties are such that the flow of metal is not disturbed. Moving imposed boundary conditions are handled by definition of a velocity for the mesh, which follows usually simple patterns, as are the descent of a hammer, closing the two halves of a matrix, etc.

For every time step an advective transport equation is solved

$$\frac{Dc}{Dt} = \frac{\partial c}{\partial t} + (\mathbf{u} - \mathbf{u}_M) \cdot \nabla c = 0 \tag{46}$$

for a scalar field c, defined in such a way that an isocurve of it identifies the interface between both materials. Here, $\mathbf{u}_M$ designs the mesh velocity assigned to impose moving boundary conditions. The solution to (46) yields the scalar field for the next time step, and the new position of the free surfaces are determined by finding again the isocurve taken as a reference for the interfaces. After that, a new solution of the constant time problem is reached $(\mathbf{u}_{t_{n+1}}, p_{t_{n+1}})$, and a further time step is performed.

The method is simple to apply, and several goals have been found: it is conservative (while most Lagrangian transient schemes are not), large time steps can be taken, for there is an acceptable approximation of the velocities on the zone to be occupied by the metal, provided by the fictitious material. Finally, very good results are obtained when compared with experimental data, as shown in the applications.

Prior to the following extension to model free surfaces of stationary processes, it is worth pointing out that on this method it is necessary to handle two materials on a single element. There are ways of doing so in an "exact" manner, *e.g.* dividing the element in sub-elements, each containing a single material. However, acceptable results are obtained by simply increasing the number of integrating points during the calculation of the element stiffness matrix, thus resulting in a simple algorithm.

The artifice of taking a free surface as an interface has been used to model those who take place in a stationary process, where the interface is moved subjected to the condition of having the velocity tangent to it. The interface calculated by integration along a streamline is used to calculate the scalar field. It has been shown to be a good practice [8] evaluating for each node as the distance of it to the curve. At the element level the scalar field will be interpolated, and different properties will be considered regarding the value of the scalar field in a given Gauss point with respect to the reference value.

By this procedure the discretized domain is not changed, this being especially interesting when modelling the problems described in the previous section, where the computation of stiffness matrices requires the domain to by axisymmetric, whereas it may actually not be so, due to the presence of free surfaces.

5. APPLICATIONS

a) Free forging

Fig. 3 reproduces the initial mesh of a cylinder that should be axially forged to have a reduction in height of 50%. This mesh is initially occupied by the metal and on its sides two rows of elements are added to contain the pseudo-material. Only a quarter of the mesh is solved, for symmetry considerations. In fig. 4 the final shape is shown (thick line), together with the intermediate shapes

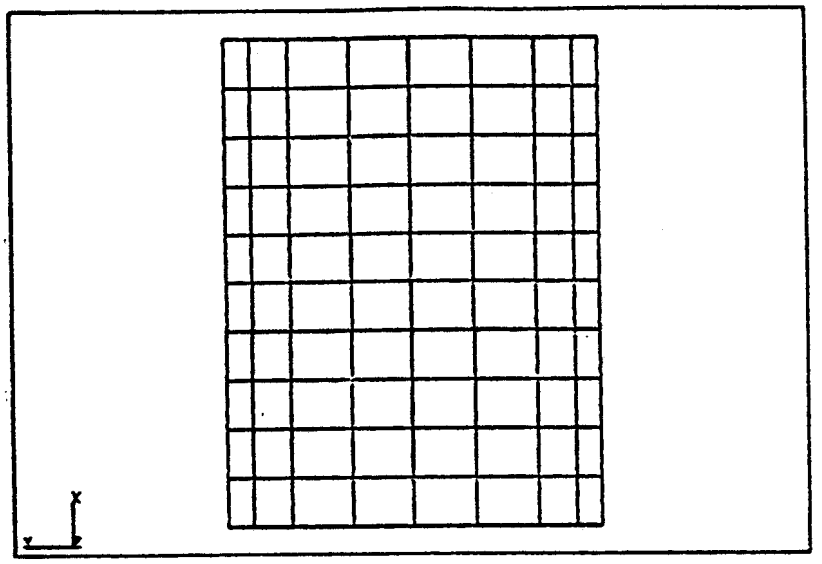

Figure 3. Free forging, initial mesh for the metal.

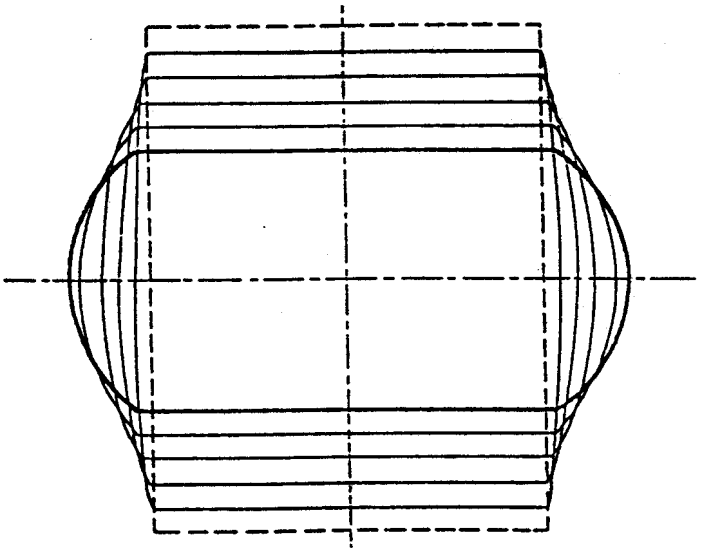

Figure 4. Free forging, final and intermediate shapes.

corresponding to every 10% reduction, plotted in fine lines. In fig. 5 *I* it is shown the experimental result, in thick line, in comparison with our results (fine line). The external contour reproduces the experimental results fairly well. A non-hardening visco-plastic model has been used. This shape has been reached after twelve constant time solutions, only one half of those which would be required in a Lagrangian description. This saving is on the most time consuming part of the

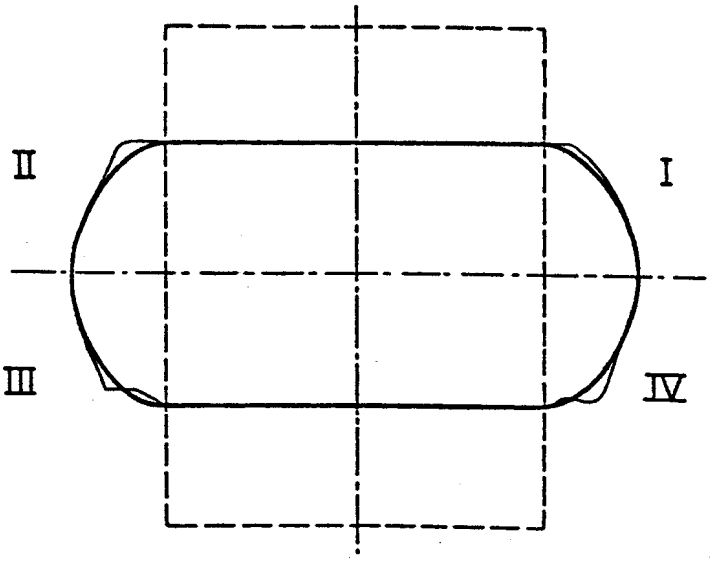

Figure 5. Free forging, experimental results [9], compared with numerical solutions.

calculation. It is due to the fact that a velocity field is given also for the zone not occupied yet by the metal, and it serves as a good approximation for the velocity of the material, when reaching this part of the domain. We also compared our results with those yielded by a Lagrangian description [9]. This is shown also in fig. 5, where *II* corresponds to a rigid–plastic model, and *III* and *IV*, to an elasto–plastic model, with eight nodes elements. In these, meshes of twenty five and fifty elements, respectively, have been used, and best results were provided by using a high order integration. The improvement in the solution when the pseudo–concentration method is applied is apparent, even using a lower number of elements: as is shown in fig. 3 we took twenty elements for the initial domain of the metal, four elements to model boundary friction and twelve to receive the flow of the metal during the deformation. This is also combined with the aforementioned saving in the number of time steps.

b) Backward extrusion

In the next example an axisymmetric backward extrusion has been modelled starting from a cylindrical piece. A reduction of 90% in height is achieved in nine time steps. In the solution of this problem sticking friction was intentionally imposed on the boundaries, in order to compare results with a similar case analyzed in reference 6. Figures. 6 to 8 compare results obtained by both methods. In view of the differences from those of the reference (dashed lines), we verified in our results the constant volume condition, and we found that it is fulfilled within 1% of error. They are also as expected for the boundary conditions imposed, even though it is not a realistic behavior. This case has also been solved considering boundary friction, by adding a layer of friction elements on the boundaries, thus

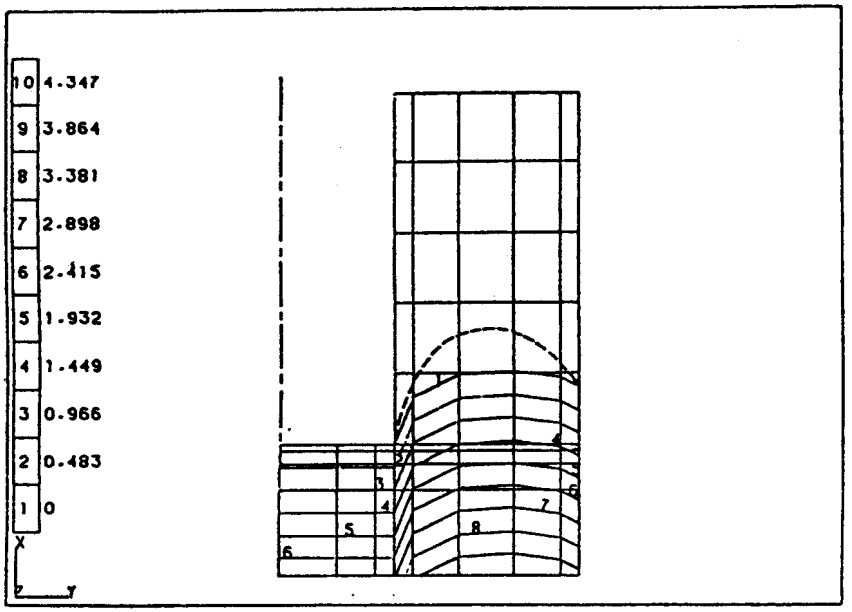

Figure 6. Backward extrusion, 30% reduction in height.

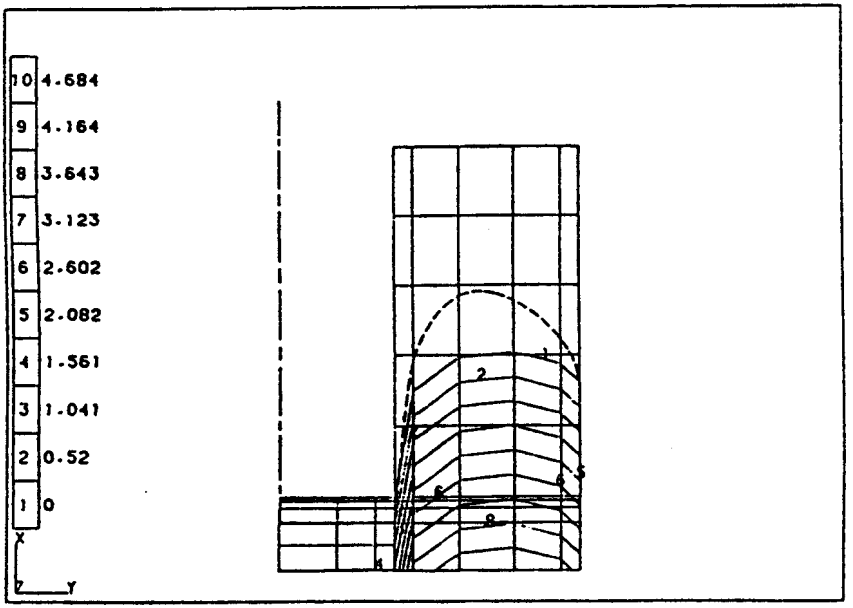

Figure 7. Backward extrusion, 60% reduction in height.

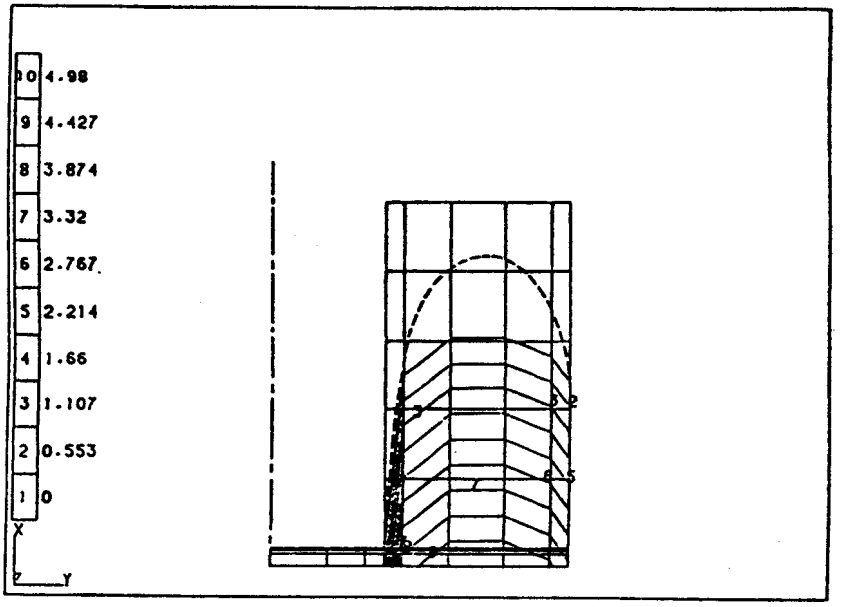

Figure 8. Backward extrusion, 90% reduction in height.

allowing a relative velocity between the metal and the matrices. The results show a similar pattern in comparison with the sticking friction case. Stresses can be seen to reduce abruptly when the material is no longer under the punch.

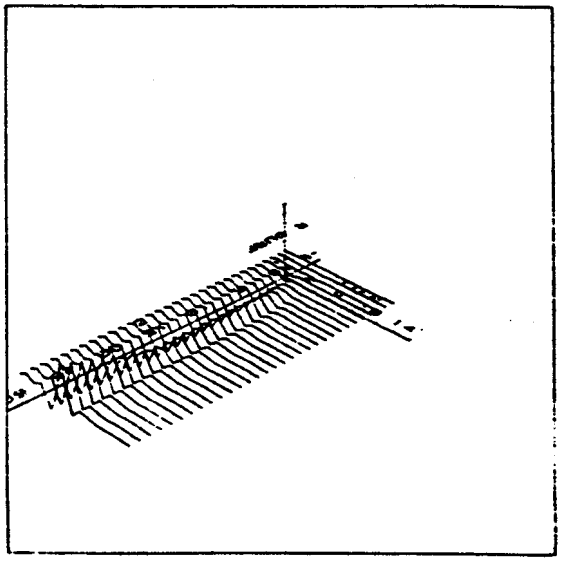

Figure 9. Direct extrusion, free suface for the interface–based algorithm.

c) Direct extrusion

The following example is presented to compare results yielded by a usual free surface procedure (*i.e.* changing nodal coordinates [10]), with the one proposed in this paper. A layer of elements with fictitious material has been added to the classical scheme to make both cases more easily comparable. Noticeable differences on the coordinates of the free surface are.found only when the mesh used is too coarse, in this case numerical solution depends strongly on the discretization. The variations of the free surface for the interface–based algorithm until convergence is obtained are plotted in fig. 9, and fig. 10 shows the maximum shear stress, which agree, as well as the other magnitudes, with the standard solution [10].

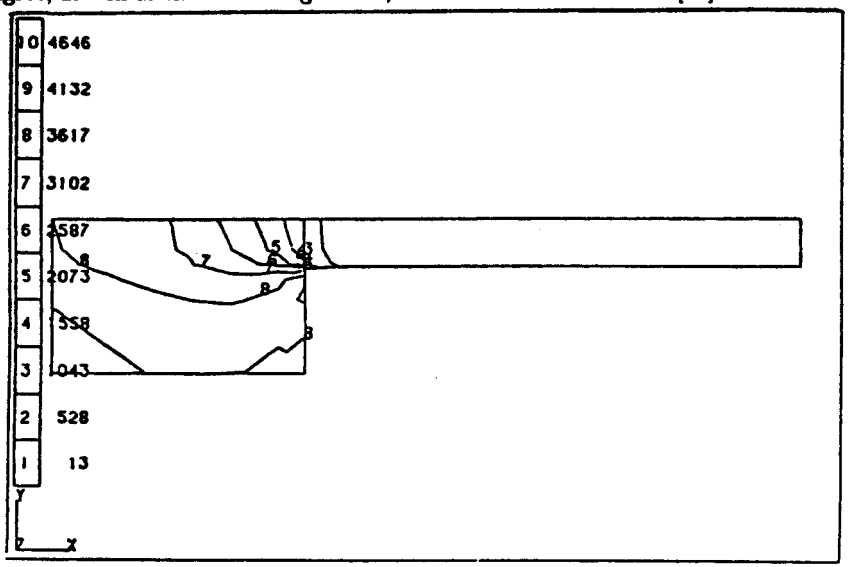

Figure 10. Direct extrusion, maximum shear stress.

d) Non–axisymmetric rolling

Rolling of pieces with circular section is a frequent process in industrial cases. In this problem the non axial symmetry is especially important due to imposed loads, and to the handling of free surfaces, which will also be non axially symmetric. We show firstly the rolling of a solid bar, with the aim of reducing its diameter. The imposed velocity is of the form

$$|\mathbf{u}| = u_0(a - b\cos\theta), \tag{47}$$

where u is in the (r, z) plane, and is tangent to the roll. Figure 11 shows the lay out of the problem. R_T and R_R are, respectively, the tube and roll radius, and ω is the roll angular velocity. The rolls are placed at 120° one each other, as shown in fig. 11. The analysis is performed with two and three terms ($\cos 3n\theta$,

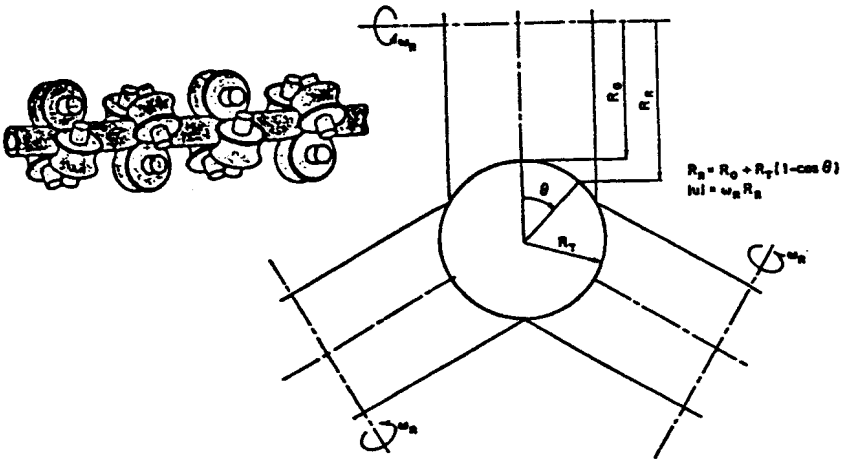

Figure 11. Rolling: lay–out.

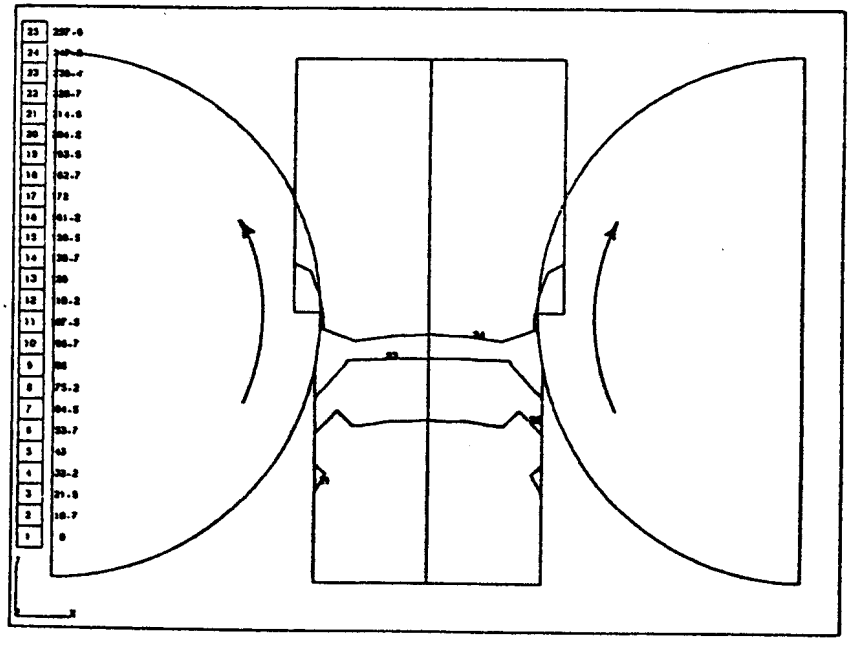

Figure 12. Rolling of a bar: velocity module, at $\theta = 0°$.

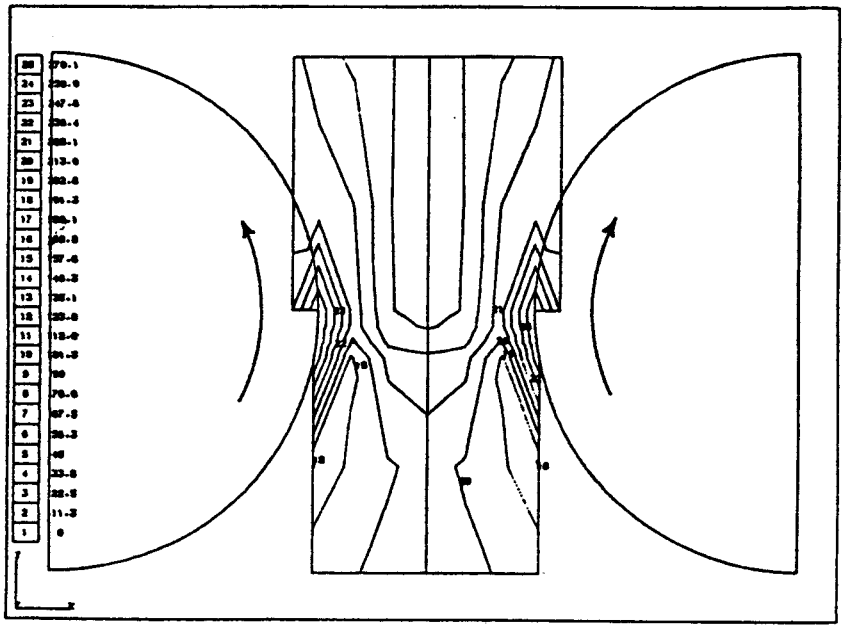

Figure 13. Rolling of a bar: velocity module, at $\theta = 32°$.

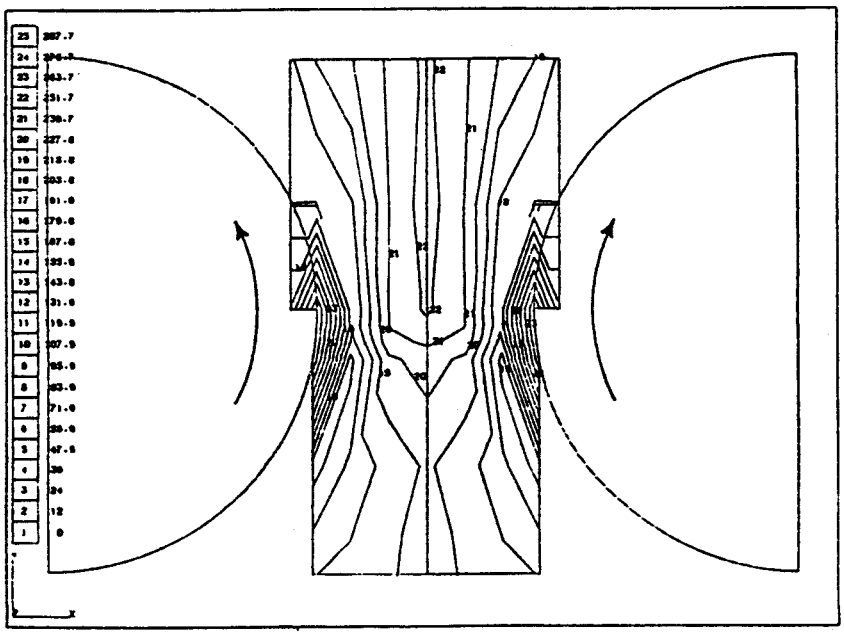

Figure 14. Rolling of a bar: velocity module, at $\theta = 54°$.

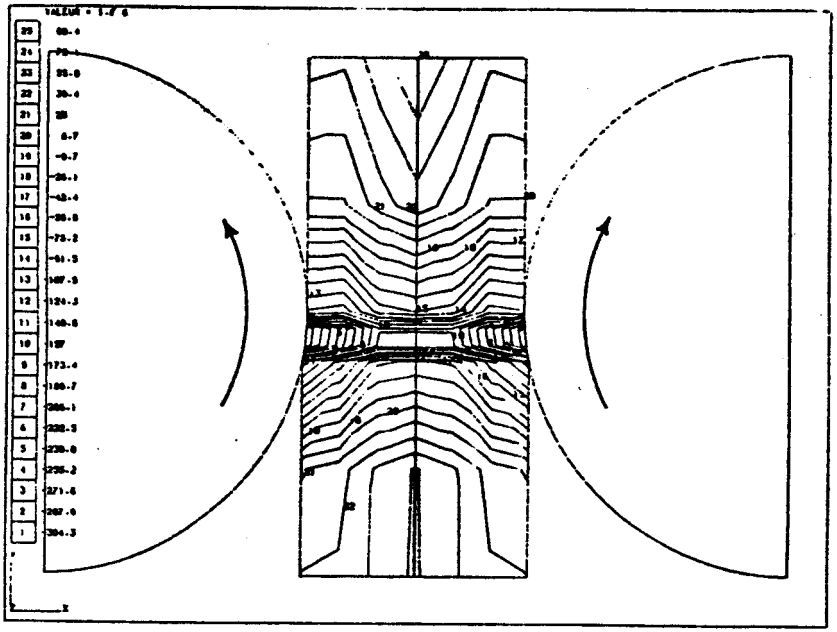

Figure 15. Rolling of a bar: axial stresses, at $\theta = 54°$.

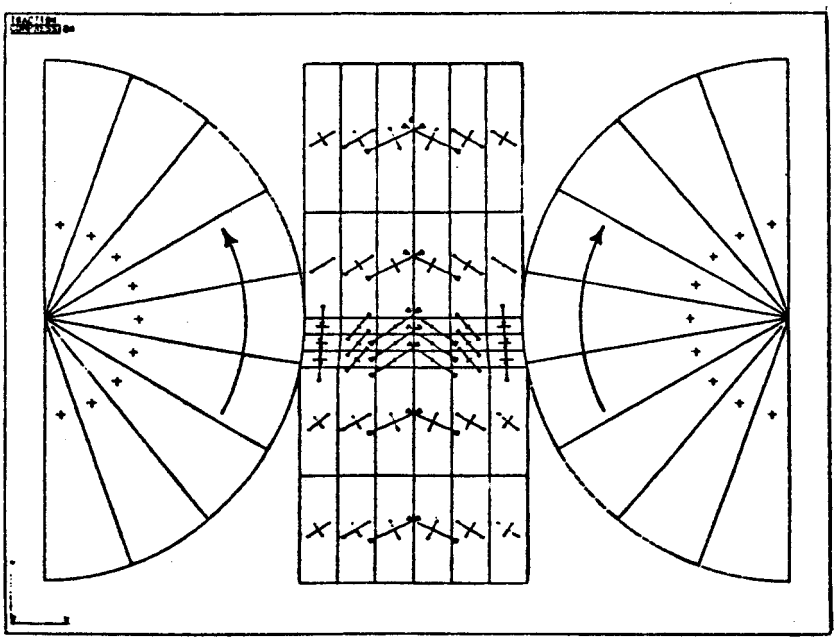

Figure 16. Rolling of a bar: stress tensors, at $\theta = 54°$.

with $n = 0, N_H$); because of the relative roll-tube magnitude considered here, negligible differences are observed between both cases. In figures 12 to 14 is clearly seen the decrease in the velocity field uniformity for increasing values of θ, from $\theta = 0°$ to $\theta = 60°$, due to the lack of axial symmetry of imposed velocities. The components of the strain tensor vanishing at the symmetry plane become important at increasing angles, then in these zones the viscosity is lower and, consequently, it appears a steep velocity gradient near the roll.

Free surfaces for this case are obtained as a function of θ, but variations are not relevant, at least compared with the diameter. In fact, free surface variations are also small for the axisymmetric case. It can be expected, however, that variations for the hollow case will be more noticeable.

Figures 15 and 16 show, respectively, the axial stresses and the stress tensors, evaluated at an intermediate angle. The effect of the roll can be clearly seen on the material tensile state.

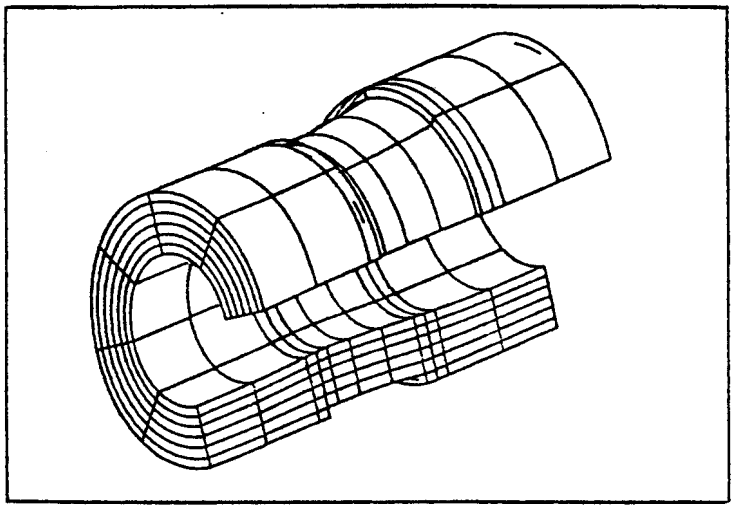

Figure 17. Tube rolling: 3-D development of discretization.

Finally we consider the rolling of a seamless tube. Fig. 17 shows a 3–D view of the solved structure. Rows of additional elements are included to contain the fictitious material at the beginning of the calculation. Later the free surface has been varying inside the discretized region, as previously described. In the angles where the equivalent load vector is evaluated for its numerical integration, it is also recombined the velocity and the integration along a streamline is performed.

Figures 18 and 19 show the isocurves of the velocity module for the extreme integration angles, for the newtonian fluid, and 20 and 21, for the viscoplastic fluid. In the linear case it is clearly seen that the material goes faster at the plane of symmetry, while the converse occurs at angles corresponding to the sides of the roll. The same happens in the non-linear case, where the high velocity gradient is seen in these angles. There are, also, high shear stresses in these places, as is shown in figure 22. On a qualitative standing, the same comments as in the

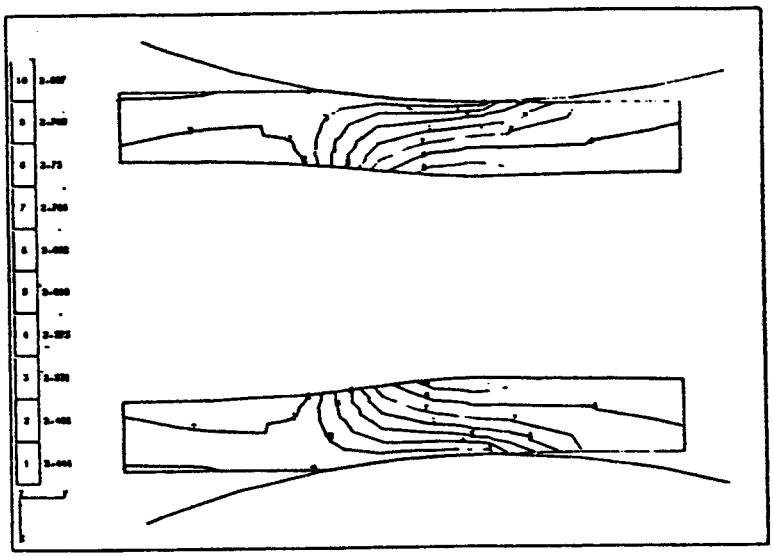

Figure 18. Tube rolling: velocity module, at $\theta = 0°$ (linear case).

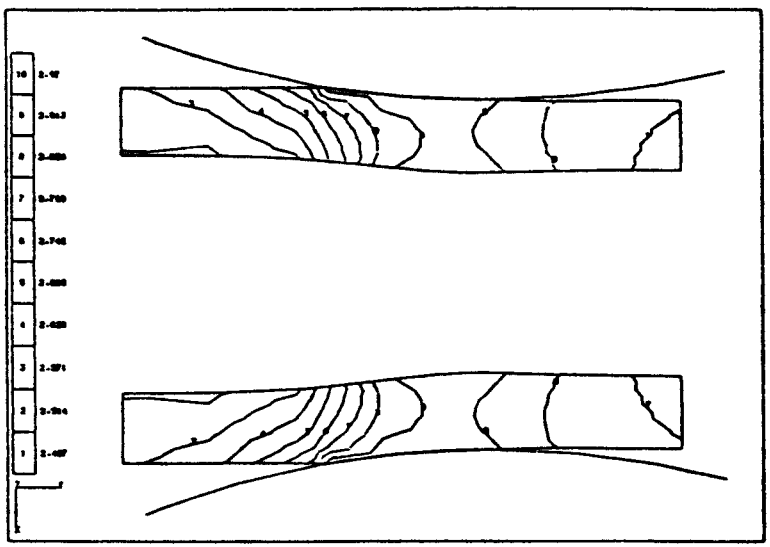

Figure 19. Tube rolling: velocity module, at $\theta = 58°$ (linear case).

axisymmetric cases can be made on the tensile state. It should be noted that the non axial symmetry is a function of the diameter relation between roll and tube.

In 2-D situations emphasis is placed on the mesh variations between initial and final configurations. Here, instead, no mesh variation is made, as required by the Fourier series expansion. The estimated shape of the mesh is reached by

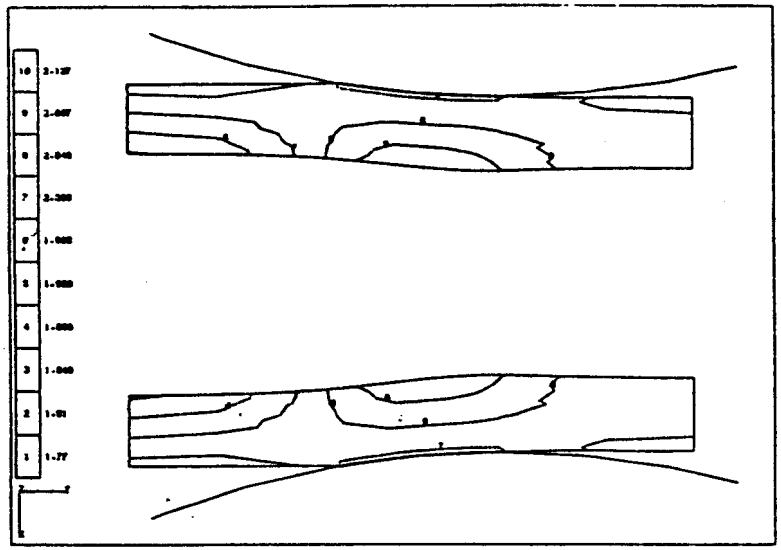

Figure 20. Tube rolling: velocity module, at $\theta = 0°$ (non-linear case).

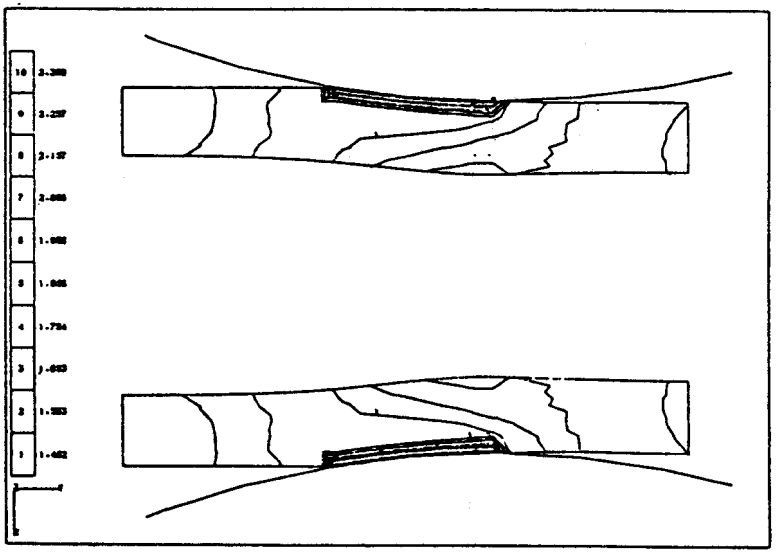

Figure 21. Tube rolling: velocity module, at $\theta = 58°$ (non-linear case).

solving an axisymmetric problem with nodal coordinates updating. Figure 23 shows the outer free surface obtained by the interface based method. In spite the variations are at least an order of magnitude greater than in the solid bar, they are hardly noticeable with respect to the tube diameter.

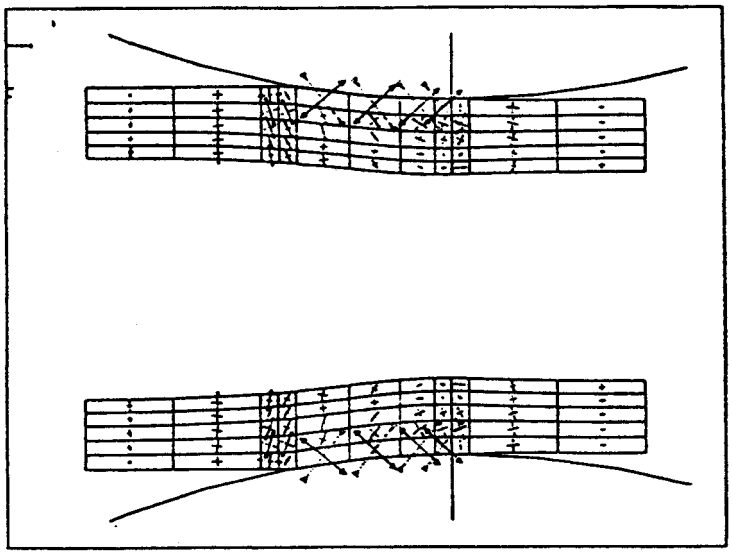

Figure 22. Tube rolling: stress tensors, at $\theta = 58°$ (non–linear case).

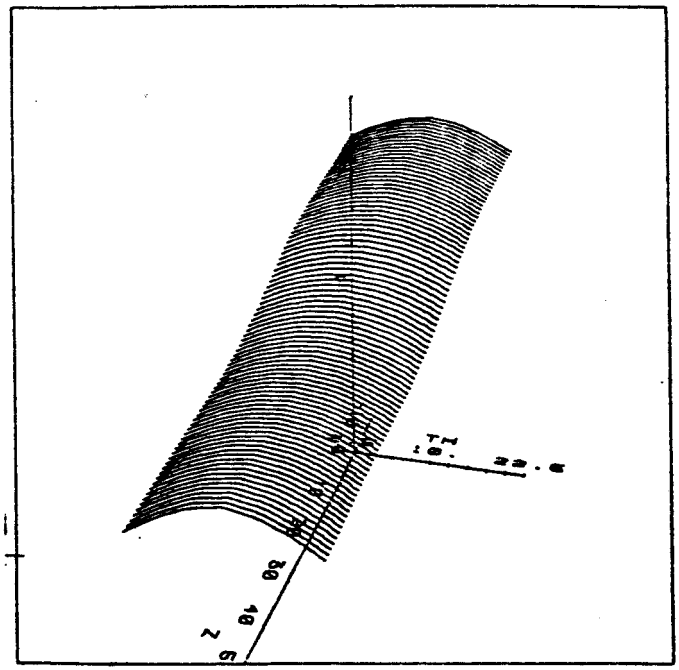

Figure 23. Tube rolling: free surface.

6. CONCLUDING REMARKS

A semi-analytical form of the flow formulation has been developed. It allows numerical simulation of non-axisymmetrically loaded processes. An incremental formulation has been necessary to derive, which in addition is a suitable scheme for modeling perfectly plastic materials, where the tangent matrix is singular and, when solved by a back-substitution procedure, convergence is very slow.

A new scheme for treating free surfaces has also been shown, which gives good results for plane configurations; its applications to non-axisymmetric problems has made it possible to include free surfaces in the semi-analytical formulation.

REFERENCES

[1] O. C. Zienkiewicz, "The Finite Element Method", Mc Graw Hill (1977).

[2] E. L. Wilson, "Structural Analysis of Axisymmetric Solids", A. I. A. A. Journal, 3, 2269-2274 (1965).

[3] P. R. Dawson & E. G. Thompson, "Finite Element Analysis of Steady State Elasto Viscoplastic Flow by the Initial Stress Rate Method", Int. J. Num. Meth. Engng.,12, 47-57 (1978).

[4] J. Cormeau, "Numerical Stability in quasi static elasto-visco-plasticity and creep in elastic solids — a unified numerical solution approach', Int. J. Num. Meth. Engng., 8, 821-845, (1974).

[5] E. G. Thompson& H. M. Berman "Steady State Analysis of Elasto-Visco-Plastic Flow During Rolling", in *Numerical Analysis of Forming Processes*, Chap.9, Pitmann et al., eds., Wiley (1984).

[6] O. C. Zienkiewicz, "Flow Formulation for Numerical Solution of Forming Processes", in *Numerical Analysis of Forming Processes*, J. F. T. Pittman, O. C. Zienkiewicz, R. D. Wood and J. M. Alexander, (eds.), Wiley, Chichester, 1984, 1-44.

[7] S. Kobayashi, "Thermoviscoplastic Analysis of Metal Forming Problems by the Finite Element Method", in *Numerical Analysis of Forming Processes*, J. F. T. Pittman, O. C. Zienkiewicz, R. D. Wood and J. M. Alexander, (eds.), Wiley, Chichester, 1984, 45-70.

[8] E. G. Thompson "Use of Pseudo-Concentrations to Follow Creeping Viscous Flows During Transient Analysis", Int. J. Num. Meth. Fluids, 6, 749-761 (1986).

[9] C. R. Boër, P. Gudmundson & N. Rebelo, "Comparison of Elastoplastic F.E.M., Rigid-Plastic F.E.M. and experiments for Cylinder Upsetting", in *Numerical Methods in Industrial Forming Processes*, J. F. T. Pittman, R. D. Wood, J. M. Alexander and O. C. Zienkiewicz, (eds.), Pineridge Press, Swansea, 1982, 217-226.

[10] H. J. Antúnez & S. R. Idelsohn, "Topics in Numerical Solution of Isothermal and Thermal-Coupled Forming Processes", Latin American Applied Research, 20, 69-83, (1990).